Additively manufactured flexure for astronomy instrumentation

Katherine Morris, Carolyn Atkins, Lucy Reynolds, James Walpole, Bart van de Vorst, Robert M. Snell, Chris Miller, Szigfrid Farkas, György Mező, Mélanie Roulet, Afrodisio Vega Moreno, Fabio Tenegi, Andrew Conley, Hermine Schnetler

Published version information

Citation: K Morris et al. 'Additively manufactured flexure for astronomy instrumentation.' Proceedings of SPIE: Advances in Optical and Mechanical Technologies for Telescopes and Instrumentation V, vol. 12188 (2022): 121880Z. Event: SPIE Astronomical Telescopes + Instrumentation 2022, Montréal, Québec, Canada, 17-23 Jul 2022.

DOI: 10.1117/12.2630180

Additively manufactured flexure for astronomy instrumentation

Katherine Morris[a], Carolyn Atkins[a], Lucy Reynolds[a], James Walpole[a], Bart van de Vorst[b], Robert M. Snell[c], Chris Miller[a], Szigfrid Farkas[d], György Mező[d], Mélanie Roulet[e], Emmanuel Hugot[e], Afrodisio Vega Moreno[f], Fabio Tenegi[f], and Hermine Schnetler[a]

[a]UK Astronomy Technology Centre, Blackford Hill, Edinburgh, United Kingdom
[b]TNO, Eindhoven, Netherlands
[c]University of Sheffield, Sir Robert Hadfield Building, Sheffield, United Kingdom
[d]Konkoly Observatory, Konkoly Thege Miklós út, Budapest, Hungary
[e]Laboratoire d'Astrophysique de Marseille, Université d'Aix-Marseille, Marseille, France
[f]Instituto de Astrofísica de Canarias, La Laguna, Tenerife, Spain

ABSTRACT

Additive Manufacturing (AM) has several potential advantages for astronomical instrumentation: particularly the ability to create custom parts with optimised geometries that cannot be produced with traditional manufacturing. The goal of the EU H2020 funded OPTICON (Optical Infrared Coordination Network for Astronomy; grant agreement 730890) A2IM (Additive Astronomy Integrated-component Manufacturing; PI H. Schnetler) project completed in June 2021, was to develop prototypes demonstrating these benefits. This paper presents the design and additive manufacture of a piezoelectric stack actuator driven, monolithic flexure for the active array of the Freeform Active Mirror Experiment (FAME). Flexure geometry had previously proved difficult to repeatedly produce and AM was considered as a potential solution. Two AM processes were used: powder bed fusion where metal powder is bonded using a laser, and binder jetting where powder is bonded using a polymer adhesive. A topology optimised, flexure hinged frame was designed based on the minimum feature size of each AM machine. This geometry was produced in Aluminium (AlSi10Mg), Titanium (Ti64Al4V) and Stainless Steel 316L. Porosity is a known issue with AM and Hot Isostatic Pressing (HIP): a post process whereby parts are subject to increased temperature and pressure was identified as a way of reducing this, thereby increasing the predictability of flexure behaviour and suitability for vacuum applications. Conformity of AM parts to their original geometry was assessed using external dimensional metrology. X-ray Computed Tomography (XCT) was used to identify internal porosity.

Keywords: Additive manufacture, 3D Printing, Piezoelectric, Actuator, Flexure, Topology optimisation, Powder bed fusion, Binder jetting, Porosity, Hot isostatic pressing, X-ray computed tomography

1. INTRODUCTION

The potential advantages of additive manufacturing for astronomy instrumentation are considerable. Consolidation of many parts into one, and creation of custom optimised geometries allow for mechanical design freedom that would be unachievable with traditional, subtractive manufacturing. ESA's "Additive Manufactured Demonstrator Telescope", [1] exhibits a complex, optimised geometry with a mass reduction of 73% compared to the original, traditionally manufactured version. Similarly, compliant mechanisms developed by CSEM [2] and BYU [3] show that alignment tolerances required by astronomical instruments can be achieved using AM. This paper will discuss the design and additive manufacture of a compliant, amplified piezoelectric actuator. Flexure hinges are of interest within astronomical instrumentation for active control of mirrors. In particular, the Horizon 2020 funded Freeform Active Mirror Experiment (FAME) is an attempt to produce a mirror with an integrated array

Further author information:
Katherine Morris: E-mail: katherine.morris@stfc.ac.uk

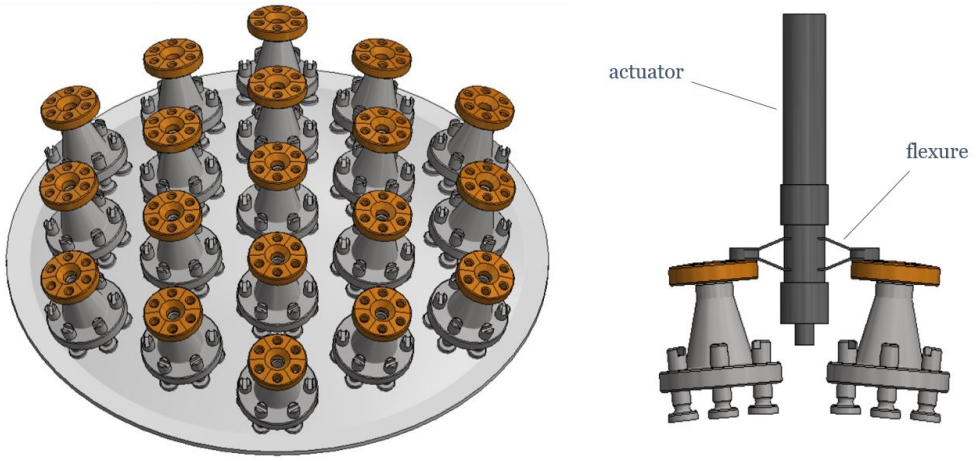

Figure 1. The FAME active array actuators are mounted between nodes to correct the mirror surface. [4]

of actuated flexures; these are controlled to change the shape of the mirror surface and correct manufacturing errors. The diameter of the optical surface is 100mm and the geometry of the active array means that there is a very limited space envelope for actuators between each of the array nodes; the displacement between node attachment points is 16.35mm. Figure 1 shows the arrangement of actuated flexures within the active mirror structure.

Previous attempts to produce the flexure geometry have included bending small steel parts into the required angles; it proved very difficult to replicate the same angles over multiple pieces. Wire Electrical Discharge Machining (EDM) was also investigated however, the fine flexure parts were very brittle due to the heat affected zone produced during the manufacturing process. AM is therefore of interest to produce functional flexures of consistent geometry that has not previously been achieved.

2. DESIGN AND OPTIMISATION

Design for AM requires a different process than for traditional manufacture: the steps taken for the flexure are shown in Figure 2 The first step was to consider materials as this influences the manufacturing process that can be used. This project focused on metals; astronomical instruments often operate under cryogenic and vacuum environments and while there are some polymers that can be used in these conditions metals were favoured to match coefficients of thermal expansion for components in an instrument assembly. The second step was to select manufacturing processes available for these materials. In the third step, design criteria which are influenced by the manufacturing process were identified. In particular, the minimum feature size was recognised as affecting the size of flexure hinge that could be produced.

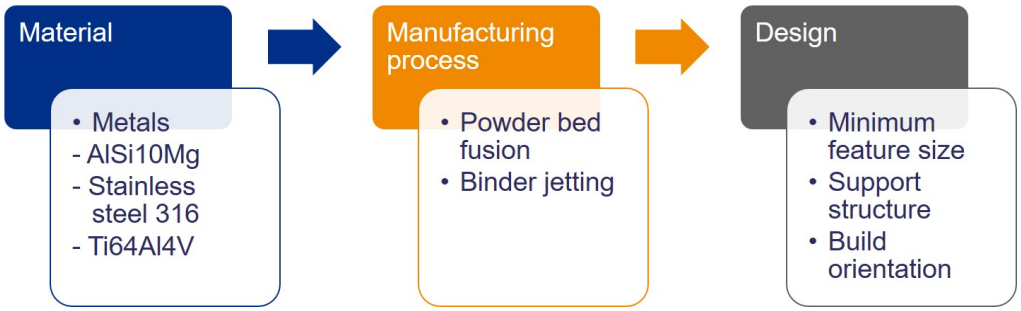

Figure 2. Flexure design process steps

2.1 Initial design

A monolithic part was designed to replicate the useful features of the FAME flexure and allow for a piezoelectric stack actuator to be directly mounted within the flexure frame as in Figure 3.

The assembly will therefore operate as shown in Figure 4: a piezoelectric actuator force is applied and an amplified resultant orthogonal force is produced.

Of particular interest are the shallow flexure arm angles at 2.3°. This angle controls the mechanical advantage of the flexure, the amplification of the actuator force according to:

$$MA = \frac{1}{sin\theta}$$

A smaller angle increases the amplification ratio, thus a manufacturing method which can consistently and accurately produce such small angles is desirable.

Figure 5 shows one of the eight circular notch hinges present in the geometry. Elastic notch hinges have been well described in the literature, including by Paros and Weisbord [5] and Lobontiu [6]. The important dimensions are minimum thickness at hinge, t and the radius of the circular notch, R. For this design which has a double-sided hinge the elastic hinge parameter can be established:

$$\beta = \frac{t}{2R}$$

A typical hinge should have $0.01 < \beta < 0.5$: below 0.01 hinges are not manufacturable and above 0.5 hinge functionality disappears. Given the overall dimensions of the flexure, a notch hinge thickness of 0.3mm was

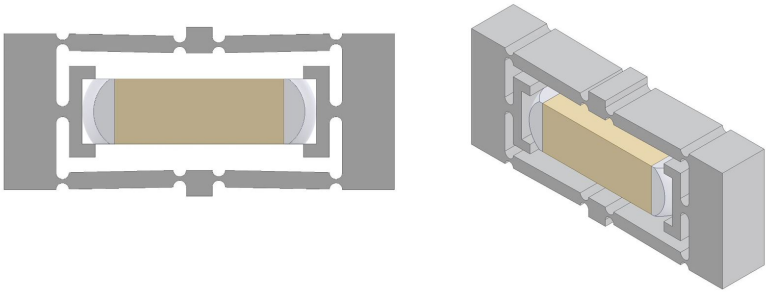

Figure 3. Flexure with integrated piezoelectric stack actuator

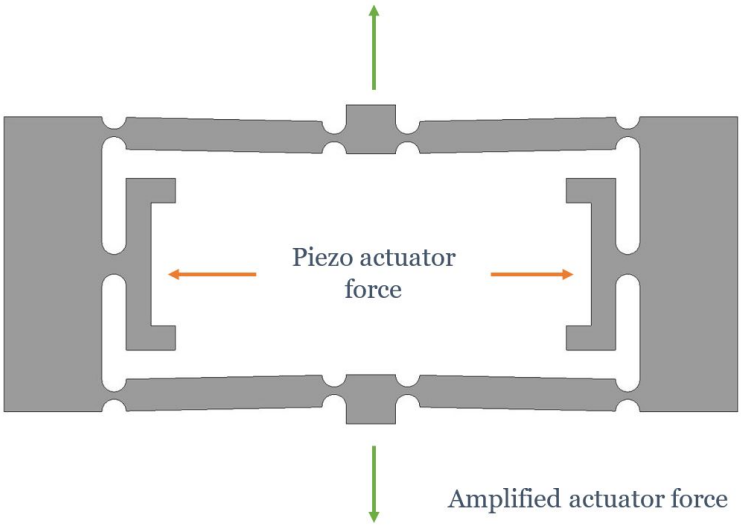

Figure 4. Piezoelectric actuator force and resultant amplified force

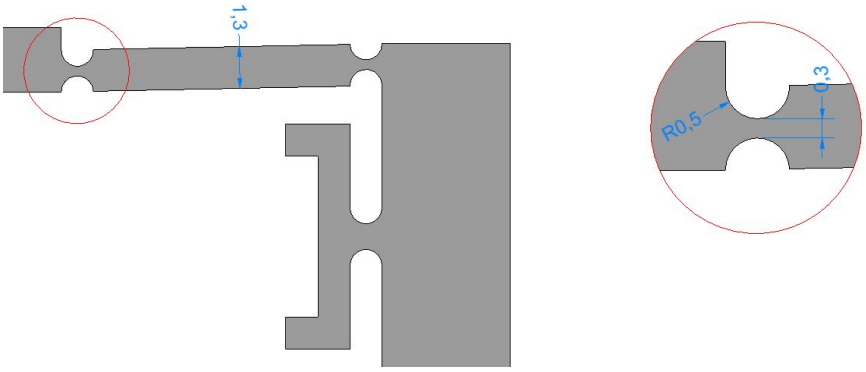

Figure 5. Flexure arm and circular notch hinge dimensions

assigned as this is manufacturable by most laser-based powder bed fusion machines. The notch radius was then based on ensuring a β value of between 0.01 and 0.5 while maintaining as small as possible a geometric footprint. A radius of 0.5mm was selected, producing a β value of 0.3. A directly piezoelectric actuated flexure would likely not be appropriate for use within the FAME active array however, the geometrical features of interest – notch hinges and flexure arm angles are still present. The realisation of these small features with AM remains of significant interest.

2.2 Topology optimisation

While the second flexure was manufacturable, it was not designed specifically for AM: the flexure could have been produced using subtractive methods such as wire EDM. The geometry was therefore redesigned using topology optimisation software to create a part more suitable for AM. Topology optimisation enables mass reduction of a part while maintaining stiffness characteristics. While mass reduction may not be advantageous for this particular part, mass saving is of great concern within both ground and space-based astronomy instrumentation. It is useful therefore to define the methodology for topology optimisation which can be used for further AM part design.

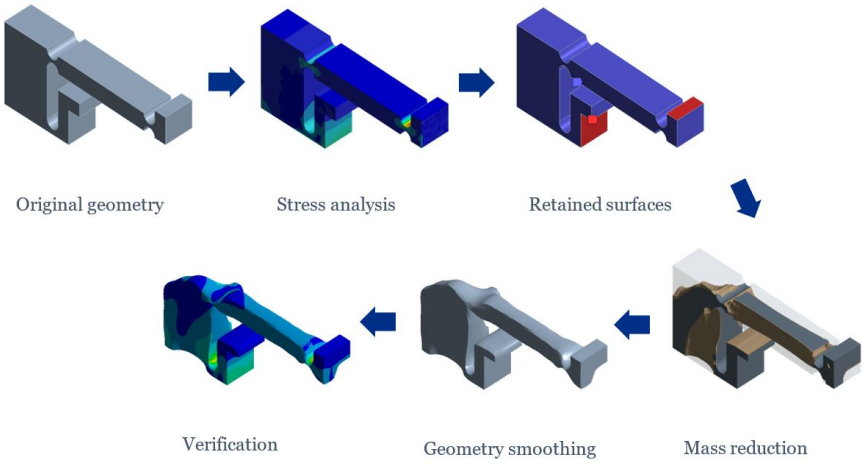

Figure 6. Topology optimisation mass reduction process steps

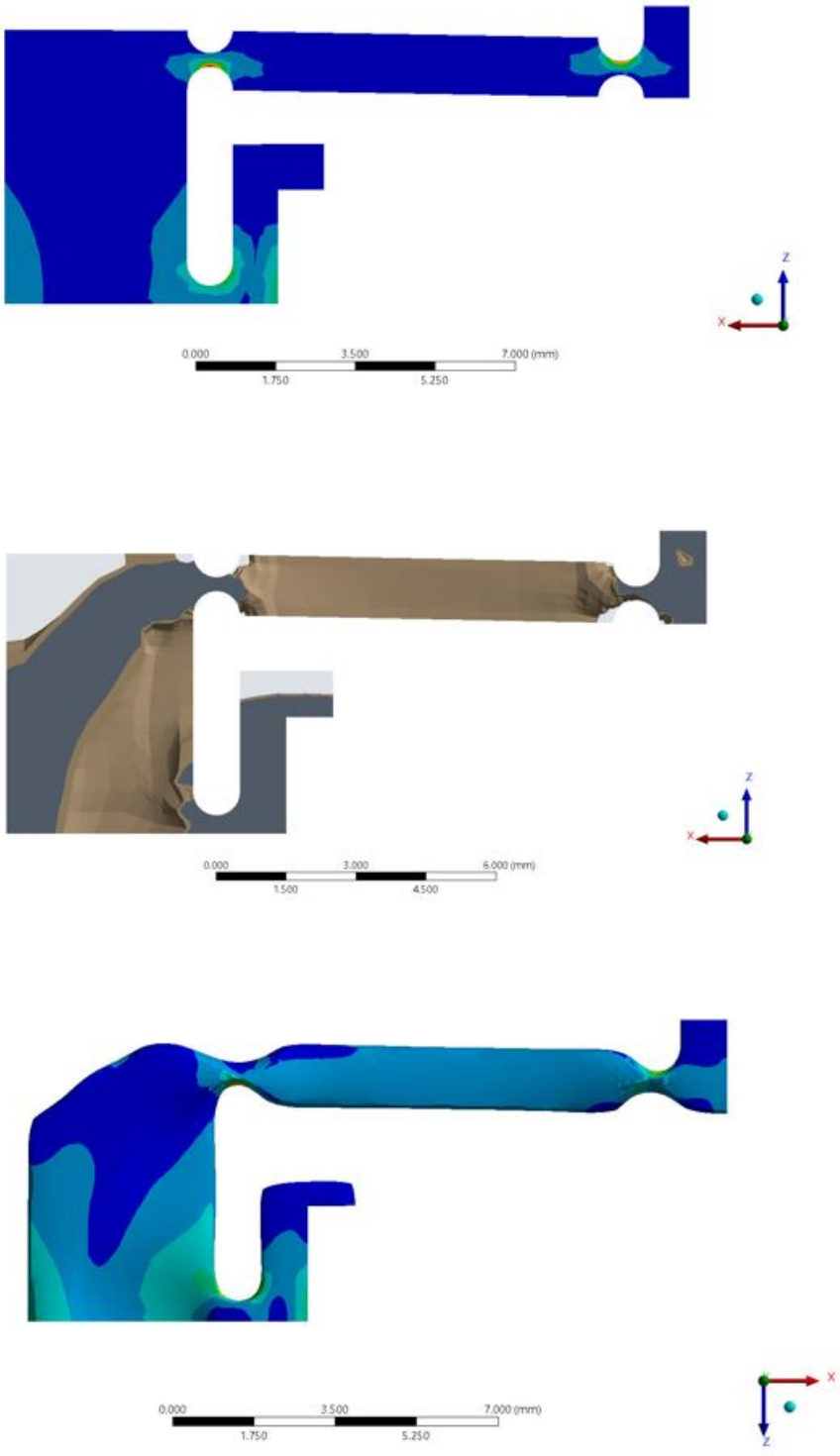

Figure 7. Topology optimisation mass reduction steps

The topology optimisation process follows the steps shown in Figure 6. A finite element stress analysis was performed on a symmetrically reduced geometry; in this case a 3-dimensional, 1/8th solid. Boundary conditions were applied: an expected force of 70N from the piezoelectric actuator and displacements and confined to specific planes. Areas to be excluded from the optimised region were then defined using the stress analysis solution shown in part 1 of Figure 7: the piezoelectric actuator mounting faces and amplified actuator metrology surface were maintained and the mass reduction was arbitrarily restricted to 50%.

Part 2 of Figure 7 shows areas where material has been removed without increasing the stress in the flexure hinges: mainly from the inactive areas with large mass. It can be noted however, that the smallest dimension of the part: thickness of the hinge features remains unaffected. Material has been removed from the inactive part of the flexure however, the flexure arms have also been affected. The software recommends reducing the mass of the arms, creating a more organic, almost bone-like twin flexure arm. This geometry is of great interest as it could certainly not be manufactured in a traditional, subtractive way. This geometry however, is not yet suitable for manufacture; there are clearly areas with sharp, angular transitions which would not be reproduced by the AM process. The geometry was therefore smoothed, while maintaining the symmetry planes and interface surfaces. Smoothing was achieved by flattening geometry peaks and by increasing the number of facets on the part surface. A verification stress simulation was performed after the smoothing operation; this gives a more realistic stress prediction as the manufacturable geometry is so different to that produced by the optimisation software. Part 3 of Figure 7 shows the secondary stress plot of the optimised geometry; it is notable that the contours indicate that the stress is distributed more evenly throughout the whole solid while remaining similar in magnitude. The geometry was then mirrored across the surfaces previously defined, creating the full flexure component as shown in Figure 8.

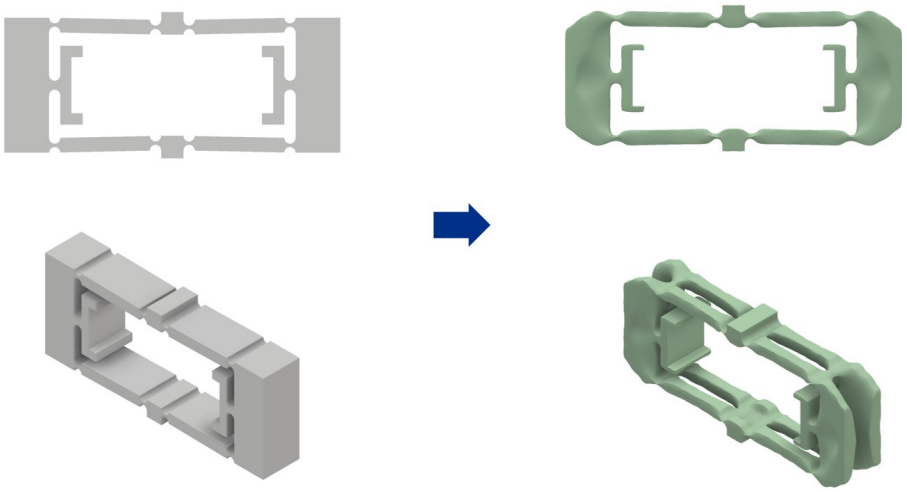

Figure 8. Initial and topology optimised flexures

3. MANUFACTURING

Both the initial and optimised flexure designs were manufactured in several materials using different manufacturing technologies. Laser Powder Bed Fusion (PBF) is a well-established process whereby successive layers of metal powder are melted into the net geometry shape by a laser. This was used to manufacture both aluminium and titanium parts. Stainless steel parts however, were produced using binder jetting: the geometry shape is created by deposition of a liquid binding agent onto successive layers of metal powder. The part is then sintered to remove the binding agent and create a solid part. Parts made using PBF often require extra material to be added during manufacture to support overhanging geometry. These supports are typically generated by software prior to manufacturing, rather than being designed into the geometry and must be removed after manufacture. Figure 9 shows the different support strategies applied to aluminium and titanium flexure parts using the same manufacturing machine.

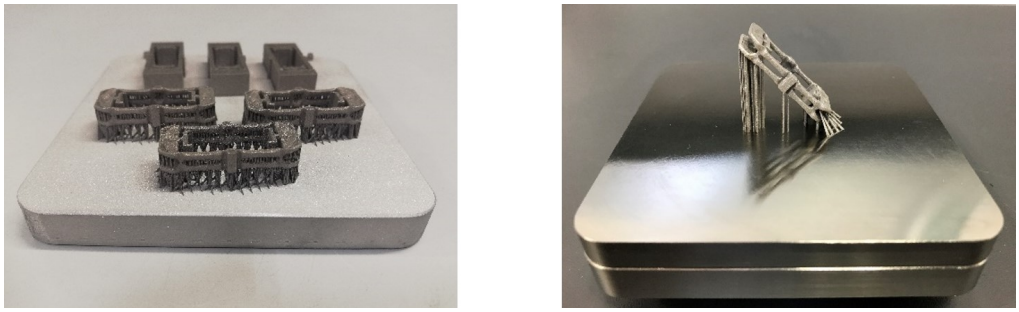

Figure 9. Powder bed fusion support structures

3.1 Post processing

Porosity is a known issue with additively manufactured parts. The microporosity shown in the Scanning Electron Microscope (SEM) images in Table 1 illustrate the porosity present in a binder jetting manufactured part, however this is typical more generally of metal powder AM parts. The pore size shown is of the range 5μm - 75μm. Hot Isostatic Pressing (HIP) is a process whereby high temperature and pressure is applied to a component to close internal pores. Near 100% density may be obtained however, any pores that reach the surface of the part will remain unaffected [7].The HIP process was of particular interest for flexures as reducing porosity would improve the predictability of the flexure behaviour, especially at the flexure hinges where fatigue is most likely to occur. HIP is also of particular interest for astronomy instrumentation as it can potentially reduce outgassing of parts under vacuum.

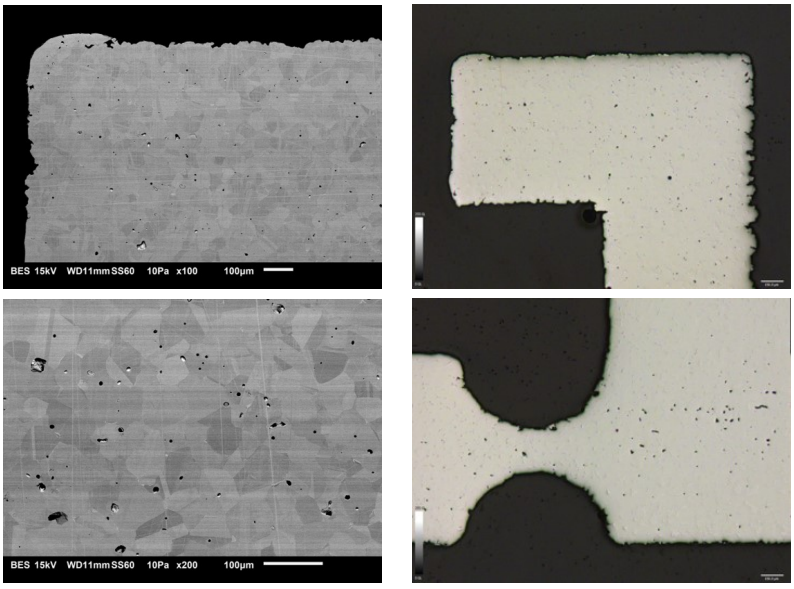

Table 1. Microporosity in binder jetting parts

4. METROLOGY

It is well documented that AM parts can have dimensional differences to the geometric model supplied for manufacture. Townsend et al. [8] found a maximum dimensional difference of -0.83% for titanium PBF test pieces. This could present an issue for assembly of mating parts. Dimensional changes can somewhat be accounted for during the design stage but if considering a post process such as HIP, these may be less predictable.

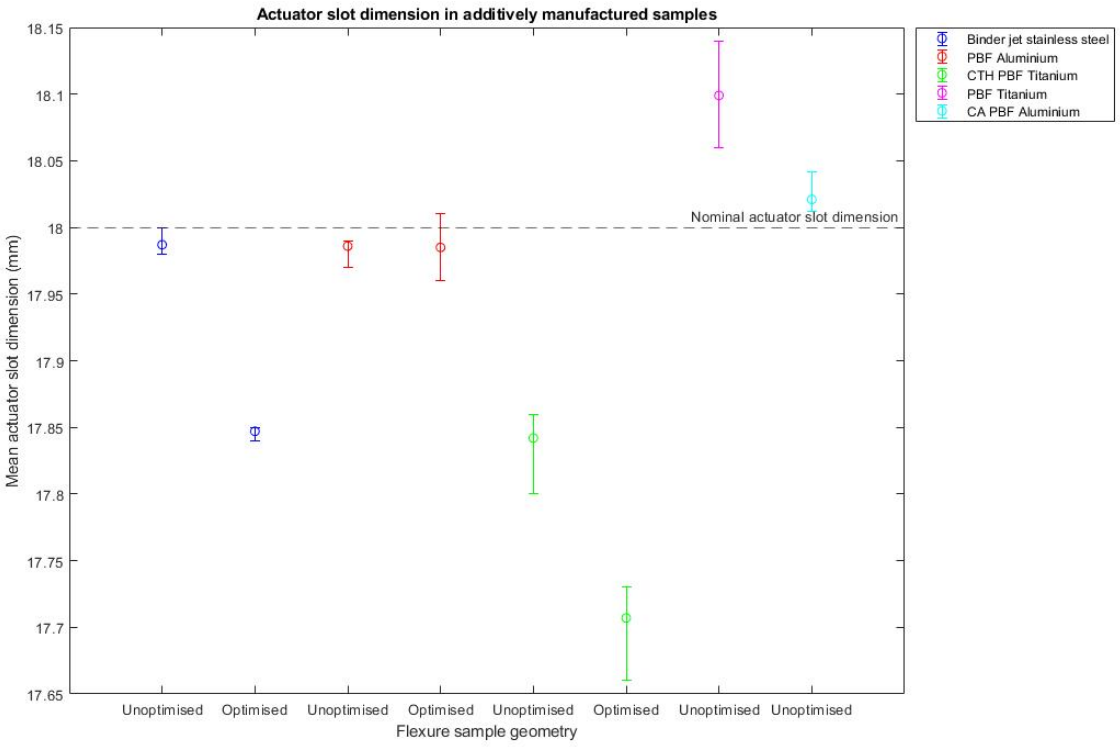

Figure 10. Variation in actuator slot dimension between additively manufactured samples.

4.1 Geometric Conformity

The part was designed to to have a piezoelectric stack actuator mounted into central slot. The dimension of this slot was therefore measured using a vernier caliper to assess if the stack actuator could be accommodated: results are shown in Figure 10

For each sample, the slot dimension should have been 18mm but the results differ for material, process and geometry: for both the binder jetting stainless steel and PBF titanium, the same process and material produced different sizes for the initial and topology optimised geometries. While an explanation for this difference is not immediately clear, support material applied to topology optimised flexures as shown in figure 9 may have some thermal effect which influences the part dimensions. It must be noted that these results do not include measurements of HIPped flexures, the differences are only shown between the two different geometries of each flexure type.

Several scanning electron microscope images were taken of both the PBF titanium and binder jetting stainless steel flexures, Figures 11 and 12 and several key dimensions were assessed, Tables 2 and 3. Overall, the dimensions of the PBF titanium parts were smaller but within 90% of the nominal geometry size; this could be corrected during the design stage. The binder jetting stainless steel dimensions are also different; build layers can be clearly seen in Figure 12 and are measured 0.17mm. This resolution is likely why the hinge thickness is larger than the model geometry. These images show that that different manufacturing processes and machine settings will produce different levels of conformity to model geometry. SEM also gives a qualitative indication of the surface roughness which is a key parameter for a flexure.

Figure 13 illustrates some potential negative features of AM components. The first image clearly shows the laser path on the surface of the part, with "pits" or depressions where the laser stops and starts: this could potentially cause outgassing issues. It may be a feature inherent to laser manufacturing processes but could be reduced through machine settings. The second image shows some surface powder grains that have not been

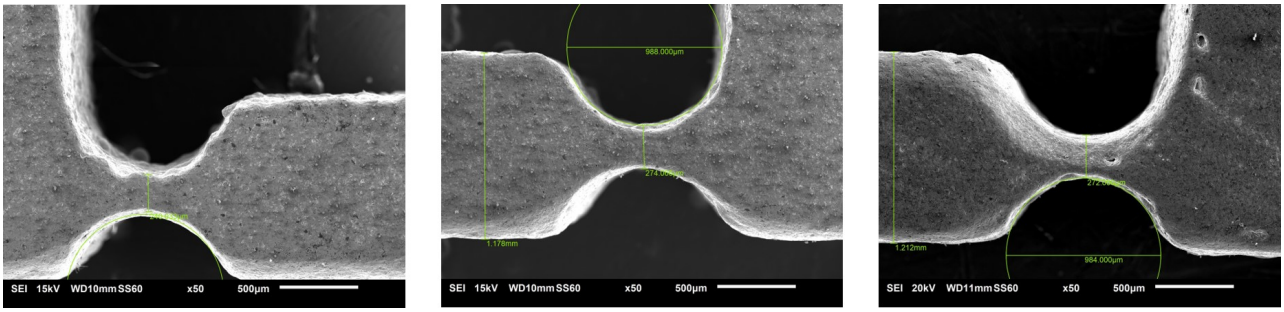

Figure 11. Powder bed fusion titanium key dimensions

	Model geometry	Laser PBF Ti64Al4V
Hinge thickness	0.3mm	0.26mm
Hinge diameter	1mm	0.986mm
Flexure arm thickness	1.3mm	0.195mm

Table 2. PBF titanium dimensions

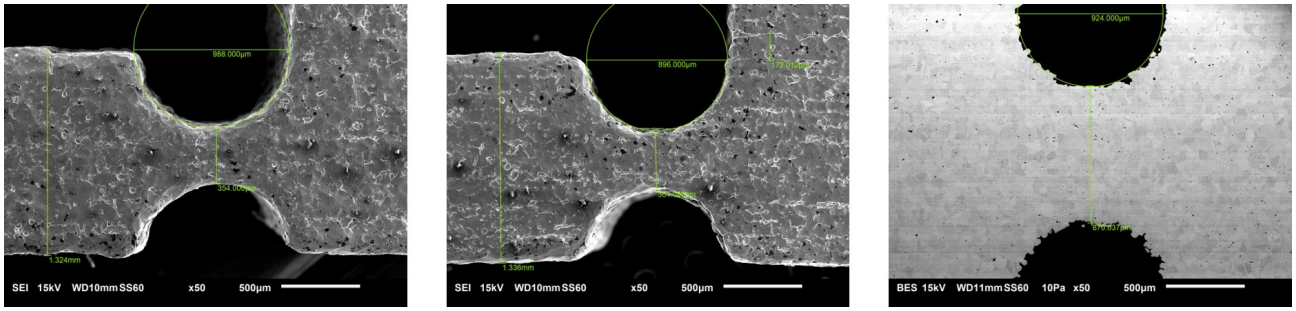

Figure 12. Binder jetting stainless steel key dimensions

	Model geometry	Binder jetting stainless steel 316L
Hinge thickness	0.3mm	0.36mm
Hinge diameter	1mm	0.936mm
Flexure arm thickness	1.3mm	0.133mm

Table 3. Binder jetting stainless steel dimensions

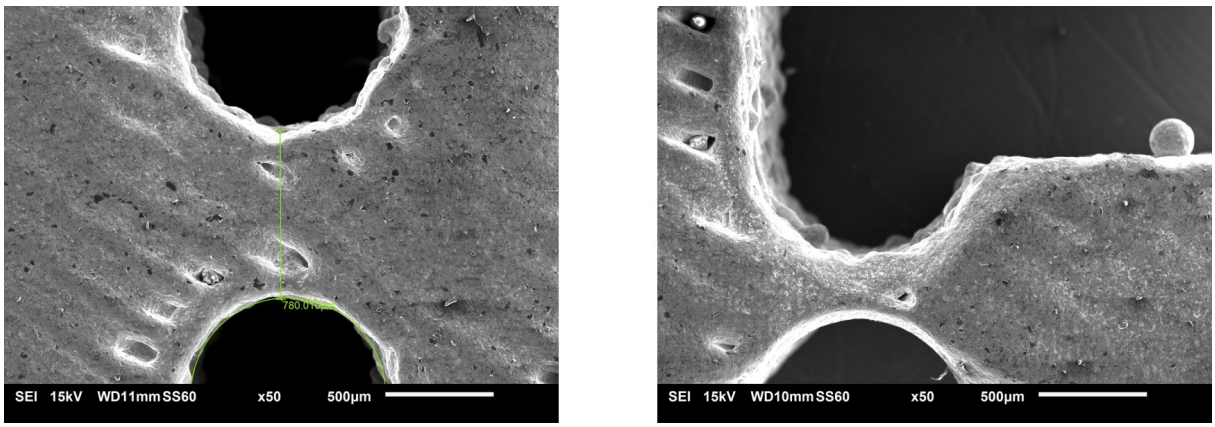

Figure 13. Laser artifact and powder inclusion on PBF component

melted into the part. These could be removed with post processing however, they may be a different material, remnants of a previous metal powder used in the manufacturing machine. It is important therefore to understand a machine's previous builds to ensure material properties.

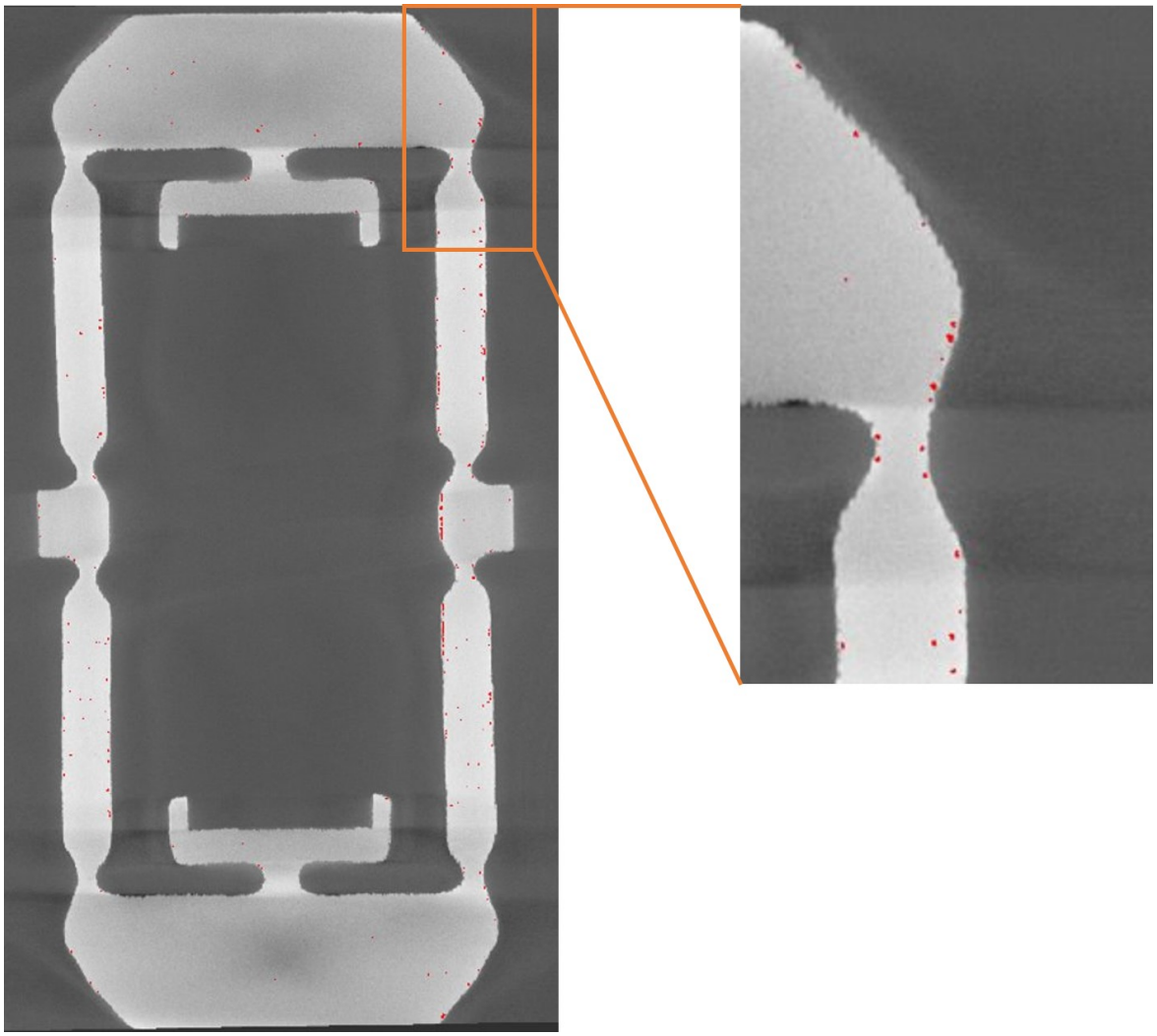

Figure 14. Pores identified on XCT image slice

4.2 Internal Porosity

As previously mentioned, porosity is a known issue with AM parts. This has the potential to cause fatigue or unpredictable mechanical behaviour in a flexure. Porosity may also give an indication of the expected outgassing if the part were to be placed under vacuum. Analysis of the flexures was therefore conducted using X-ray Computed Tomography (XCT). XCT involves using X-ray equipment to create a series of image slices through the depth of the part. Thus, a 3-dimensional image of both the exterior and interior can be created. Figure 14 shows the attenuation of X-rays through different media of the part: internal porosity appears as dark spots; these have been highlighted in red for clarity. It is possible to see pores that appear to follow external geometry of the part. This is likely "sub-contour porosity" caused by the difference in melt characteristics between the "contour" and "raster" laser scans To detect pores, MATLAB's edge detection function was used. This uses the Sobel Operator to approximate the intensity gradient at each point in the image. The function then uses a threshold to binarize the image into edges and non-edges. This threshold is initially calculated using just the part of the image containing the sample then it is manually adjusted to find the value which most realistically identifies pores. Any edges detected outside the area of the image containing the sample are removed. It is important to be aware therefore that the accuracy of pore identification is limited and that it is more useful to focus on the overall trends in porosity between the different geometries. Table 1 shows broadly the number of pores in the 50% mass reduced flexures reduced by around half.

Sample	Number of pores	Percentage porosity	Median pore size (μm^3)
Stainless steel	80000	0.30%	34000
Optimised stainless steel	46000	0.45%	45000
Aluminium	42000	0.26%	55000
Optimised Aluminium	23000	0.08%	24000

Table 4. Non-HIPped flexure porosity measurements

To reduce the uncertainty associated with the identification of pores using MATLAB, the application of a more specialised software package was investigated. AVIZO is a dedicated XCT and microscopy image analysis tool which could improve porosity measurements, particularly the comparison of non-HIPped and HIPped flexures. Figure 15 shows the difference in pore identification between MATLAB and AVIZO. While a full analysis has not yet been completed, preliminary qualitative observation of an aluminium flexure suggest a reduction in porosity post-HIP.

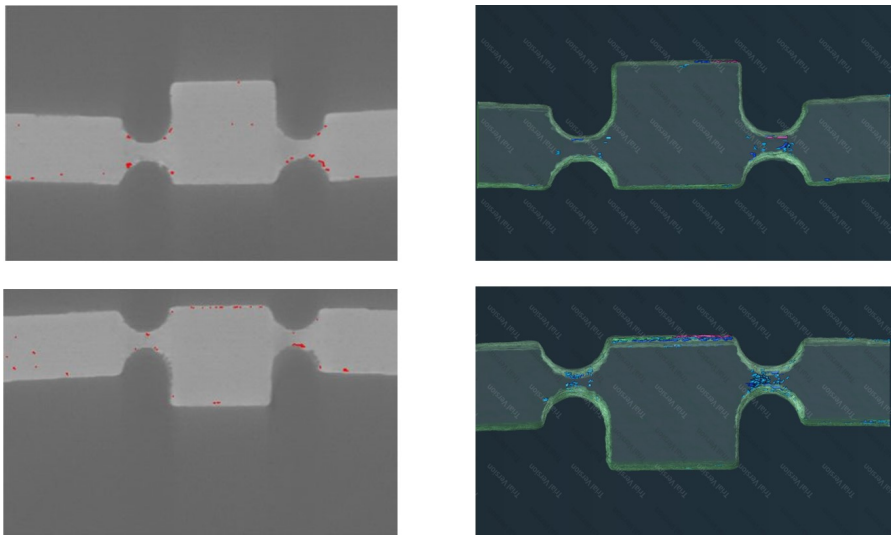

Figure 15. MATLAB and AVIZO pore identification on flexure

5. CONCLUSION

The aim of this project was to investigate the utility of additive manufacture for flexure geometries. Geometry design was iterated to replicate the FAME active array flexure and create a part that was suitable for AM. The final design: a topology optimised flexure with integrated piezoelectric actuator was manufactured in aluminium AlSi10Mg and Titanium Ti64Al4V using laser powder bed fusion, and in stainless steel 316L using binder jetting. HIP was performed on the flexures to reduce internal porosity. Dimensional metrology was performed on the flexures to investigate their conformity to model geometry. Overall the flexures displayed reduced sizes of key dimensions with the exception of the binder jetting stainless steel hinge thickness which was larger due to build layer resolution. The internal porosity was evaluated using XCT and MATLAB image analysis, with a maximum porosity of 0.45% for binder jetting stainless steel 316L and a minimum of 0.08% for PBF aluminium AlSi10Mg. While the porosity difference due to HIP has not yet been quantified, preliminary investigation using AVIZO software suggests a reduction.

ACKNOWLEDGMENTS

This project has received funding from the European Union's Horizon 2020 research and innovation programme under grant agreement # 730890. This material reflects only the authors views and the Commission is not liable for any use that may be made of the information contained therein. K. Morris & C. Atkins acknowledge the

UKRI Future Leaders Fellowship program, grant # MR/T042230/1, for enabling delivery of this research. The authors acknowledge the generous support of David Bogg at the STFC - Campus Technology Hub for enabling the production of prototype flexures.

References

[1] European Space Agency, "Printing a telescope for space." European Space Agency, 11 March 2020 https://www.esa.int/Enabling_Support/Space_Engineering_Technology/Printing_a_telescope_for_space. (Accessed: 25 April 2022).

[2] Kiener, L., Saudan, H., Cosandier, F., Perruchoud, G., Pejchal, V., Lani, S., and Rouvinet, J., "Additive manufacturing: innovative concepts of compliant mechanisms," in [*Advances in Optical and Mechanical Technologies for Telescopes and Instrumentation IV*], Navarro, R. and Geyl, R., eds., **11451**, 535 – 542, International Society for Optics and Photonics, SPIE (2020).

[3] Merriam, E. G., amd S. P. Magleby, J. E. J., and Howell, L. L., "Monolithic 2 dof fully compliant space pointing mechanism," *Mechanical Sciences* **4**, 381–391 (2013).

[4] Aitink-Kroes, G., Agócs, T., Black, C. M. M., Farkas, S., Lemared, S., Bettonvil, F., Montgomery, D., Marcos, M., Jaskó, A., van Duffelen, F., Challita, Z., Fok, S., Kiaeerad, F., Hugot, E., Schnetler, H., and Venema, L., "Fame: freeform active mirror experiment," in [*Advances in Optical and Mechanical Technologies for Telescopes and Instrumentation II*], Ramón Navarro, J. H. B., ed., *Proc. SPIE* **9912** (2016).

[5] Paros, J. M. and Weisbord, L., "How to design flexure hinges," *Machine Design* **37**, 151–157 (1965).

[6] Lobontiu, N., [*Compliant Mechanisms*], CRC Press, Abingdon (2002).

[7] du Plessis, A. and Macdonald, E., "Hot isostatic pressing in metal additive manufacturing: X-ray tomography reveals details of pore closure," *Additive Manufacturing* **34**, 101–191 (2020).

[8] Townsend, A., Racasan, R., Leach, R., Senin, N., Thompson, A., Ramsey, A., Bate, D., Woolliams, P., Brown, S., and Blunt, L., "An interlaboratory comparison of x-ray computed tomography measurement for texture and dimensional characterisation of additively manufactured parts," *Additive Manufacturing* **23**, 422–432 (2018).